

DETECTION PERFORMANCE FOR DISCRETE TEST STATISTICS. APPLICATION TO LOW-FLUX IMAGERY.

André Ferrari[†] and Jean-Yves Tourneret^{*}

[†] LUAN, Université de Nice-Sophia-Antipolis, 06108 Nice cedex 2, France

^{*} ENSEEIHT/TéSA, 2 rue Charles Camichel, BP 7122, 31071 Toulouse cedex 7, France

ferrari@unice.fr, jean-yves.tourneret@tesa.prd.fr

ABSTRACT

This communication studies a measure of detection performance for testing binary hypotheses by using discrete test statistics. This measure is the area under the receiver operating characteristics. This theory is applied to the detection of changes in low-flux images with the Neyman Pearson detector. An approximation of this measure can be derived. It allows to define a specific signal to noise ratio for the low-flux detector.

1. INTRODUCTION

Bayesian decision theory has received much attention in the signal processing literature (see [1] and references therein). Bayes detection strategy requires to define costs associated to correct and wrong decisions as well as prior probabilities for each hypothesis. When such information is not available, most common tests (such as the Neyman-Pearson test) try to minimize appropriate functions of the probability of non-detection (PND) and the probability of false alarm (PFA). In such situations, the Receiver Operating Characteristic (ROC) is a very common measure of performance for the test. The ROC represents the probability of detection (PD) as a function of the PFA. As a consequence, the PD can be computed from the ROC, for any value of PFA. The PD can then be used to specify the test performance.

However, specifying the exact value of PFA in a practical application can be a real problem. For this reason, some global measure of performance can be preferred. Barrett *et al.* proposed to measure the performance of a test by computing the area under the ROC, referred to as AUC [2]. Different expressions of AUC were derived in [2] by assuming known some characteristics regarding the test statistic. For instance, expressions of AUC were derived in the Gaussian context or for known moments of the test statistics. All material presented in [2] was obtained for continuous test statistics. The AUC was used in [3] as a measure of performance for targets detection in active imagery. This paper addresses the problem of determining the AUC when the test statistic is a purely discrete random variable. The concept of AUC for a discrete test statistic is formulated in section 2. Expressions of AUC as functions of probability masses and characteristic functions are presented in sections 3 and 4. Section 5 derives a closed form-expression of AUCs for a low flux detection problem. Section 6 studies an approximation of AUC for the Neyman-Pearson test obtained by expanding in Taylor series the moment-generating function of the test statistic. Theoretical results are validated by simulations. Conclusions are reported in section 7.

2. PROBLEM FORMULATION

We consider a standard binary hypothesis problem which can be formulated as follows

$$H_0 \text{ rejected if } T \geq \zeta, \quad H_0 \text{ accepted if } T < \zeta. \quad (1)$$

where $x = (x_1, \dots, x_N)$ is the observation vector, T is the test statistic and ζ is a threshold depending on the PFA. This paper assumes that T is a purely discrete random variable taking its values in the countable set $E = \{t_j, j \in J\}$ under both hypotheses H_0 and H_1 . By denoting as $p_i(t_j) = P[T = t_j | H_i]$ the probability mass of T at point t_j under hypothesis H_i , the PFA and PND for the test (1) can be classically defined as follows:

$$PFA = \sum_{t_j \geq \zeta} p_0(t_j), \quad PND = \sum_{t_j < \zeta} p_1(t_j). \quad (2)$$

As a consequence, in the (PFA, PND) plane, there is a countable number of operating points corresponding to all possible values of ζ . For instance, consider a test statistic T distributed according to a Bernoulli distribution under hypotheses H_0 and H_1 . In this case $E = \{0, 1\}$ and the ROC reduces to three operating points $(0, 0)$, $(p_0(1), p_1(1))$ and $(1, 1)$ corresponding to the three following situations $\zeta \leq 0$, $\zeta \in]0, 1[$ and $\zeta > 1$.

The idea of using the entire ROC curve to define a detection performance measure was suggested in [2]. Different expressions of the AUC were derived in the case of a continuous test statistic T . This paper addresses the problem of determining the AUC when T is a discrete random variable under hypotheses H_0 and H_1 .

3. AUC VERSUS PROBABILITY MASSES

3.1. Bernoulli test statistics

This simple example is interesting since it provides a simple expression of the AUC. The AUC can be computed as the sum of a triangle area and a trapeze area:

$$AUC = \frac{1}{2} + \frac{p_1 - p_0}{2}, \quad (3)$$

where $p_1 = p_1(1)$ and $p_0 = p_0(1)$. This equation shows that the detection performance is an increasing function of $p_1 - p_0$ which equals $\frac{1}{2}$ when $p_1 = p_0$ (the worst case) and 1 when $p_1 - p_0 = 1$ (the best case).

3.2. Poisson test statistic

The probability masses of the Poisson distribution under both hypotheses are denoted as $P[T = j|H_i] = \lambda_i^j e^{-\lambda_i} / j!$. Straightforward computations allow to express the AUC as follows:

$$\text{AUC} = 1 - e^{-(\lambda_0 + \lambda_1)} \text{AUC}_1 + \frac{1}{2} e^{-(\lambda_0 + \lambda_1)} \text{AUC}_2, \quad (4)$$

where

$$\text{AUC}_1 = \sum_{k=0}^{\infty} \sum_{i=0}^k \frac{\lambda_0^k \lambda_1^i}{k! i!}, \quad \text{AUC}_2 = \sum_{k=0}^{\infty} \frac{\lambda_0^k \lambda_1^k}{k! k!}. \quad (5)$$

Appendix A shows that (4) can be simplified into the following closed-form expression:

$$\text{AUC} = 1 - e^{-(\lambda_0 + \lambda_1)} \sum_{l=0}^{\infty} \left(\frac{\lambda_0}{\lambda_1} \right)^{l/2} I_l(2\sqrt{\lambda_0 \lambda_1}) + \frac{1}{2} e^{-(\lambda_0 + \lambda_1)} I_0(2\sqrt{\lambda_0 \lambda_1}), \quad (6)$$

where $I_l(z)$ is the modified Bessel function of the first kind of order l [4].

4. AUC VERSUS CHARACTERISTIC FUNCTIONS

The AUC can be expressed as a function of the characteristic functions of T under hypotheses H_0 and H_1 . More precisely, by denoting as $\psi_k(u) = E[e^{-2i\pi u T} | H_k]$ the characteristic function of T under hypothesis H_k , the following result can be obtained [2]:

$$\text{AUC} = \frac{1}{2} + \frac{1}{2i\pi} \mathcal{P} \int_{\mathbb{R}} \psi_0(u) \psi_1^*(u) \frac{du}{u}, \quad (7)$$

where \mathcal{P} indicates that the singular integral must be interpreted as a Cauchy principal value. This expression is interesting when the probability masses of T have no simple expressions under hypotheses H_0 and H_1 (see section 5 for an example). However, the computation of the Cauchy principal value can be a problem. This section explains how (7) can be used to compute AUC in the two previous cases.

4.1. Bernoulli test statistic

The characteristic functions can be easily computed in this trivial example:

$$\frac{\psi_0(u) \psi_1^*(u)}{u} = \frac{p_0 p_1 + q_0 q_1}{u} + p_0 q_1 \frac{e^{-2i\pi u}}{u} + q_0 p_1 \frac{e^{2i\pi u}}{u}. \quad (8)$$

By using the standard results $\mathcal{P} \left(\frac{du}{u} \right) = 0$ and $\int \frac{e^{iu x}}{u} du = (i\pi) \text{sgn}(x)$, where $\text{sgn}(x)$ is the signum function and $\text{sgn}(0) = 0$, the AUC can be computed by using (7) and yields the same result as in (3).

4.2. Poisson test statistic

This example presents the methodology which can be applied to compute the Cauchy principal value of (7). The characteristic functions of T under both hypotheses can be computed (we use the same notations as in section 3.2) and lead to:

$$\psi_0(u) \psi_1^*(u) = \frac{\exp[\lambda_0 e^{-2i\pi u}] \exp[\lambda_1 e^{2i\pi u}]}{e^{\lambda_0 + \lambda_1}}. \quad (9)$$

By expanding into Taylor series the two last exponentials appearing in the right hand side of (9), the following results can be obtained:

$$\frac{\psi_0(u) \psi_1^*(u)}{u} = e^{-(\lambda_0 + \lambda_1)} \sum_{k=0}^{\infty} \sum_{l=0}^{\infty} \frac{\lambda_0^k \lambda_1^l}{k! l!} \frac{e^{2i\pi(l-k)u}}{u}. \quad (10)$$

Consequently, the AUC can be expressed as

$$\text{AUC} = \frac{1}{2} + \frac{1}{2} e^{-(\lambda_0 + \lambda_1)} \sum_{k=0}^{\infty} \sum_{l \neq k}^{\infty} \frac{\lambda_0^k \lambda_1^l}{k! l!} \text{sgn}(l - k), \quad (11)$$

which reduces to (6) after straightforward simplifications.

5. APPLICATION TO LOW-FLUX IMAGERY

The evaluation of detection performance by using the AUC is illustrated in this section by a low-flux detection problem. This problem occurs for example in extra-solar planet detection from photometric signals. In this case, the N recorded data X_n are distributed according to Poisson distributions under both hypotheses:

$$H_0 : X_n \sim \text{Poisson}(f), \quad H_1 : X_n \sim \text{Poisson}(f + h\alpha_n), \quad (12)$$

where α_n denotes the point spread function of the system (with the normalization condition $\sum_{n=1}^N \alpha_n = 1$). The Neyman-Pearson detector for this problem expresses as:

$$H_0 \text{ accepted if } T = -h + \sum_{n=1}^N \beta_n X_n < \zeta, \quad (13)$$

where $\beta_n = \log(1 + \frac{h}{f} \alpha_n)$.

Eq. (13) shows that the distribution of $T + h$ is a mixture of discrete Poisson distributions. Unfortunately, the determination of the probability masses of T under both hypotheses is very complicated in the general case. The performance of this test was studied in [5] under *high-flux* assumption when f is large (by using Gaussian approximations).

This section determines the performance of the Neyman-Pearson detector (12) in terms of AUC under the *low-flux* assumption (which precludes the Gaussian approximations). The AUC can be computed since the characteristic functions of T under both hypotheses can be easily derived from (7). Indeed, by using the independence property between the random variables X_n , the following results are obtained:

$$\begin{aligned} \frac{\psi_0(u)}{e^{-2i\pi u h}} &= e^{-Nf} \exp\left(\sum_{n=1}^N f e^{-2i\pi \beta_n u}\right), \\ \frac{\psi_1^*(u)}{e^{2i\pi u h}} &= e^{-Nf-h} \exp\left(\sum_{n=1}^N (f + h\alpha_n) e^{2i\pi \beta_n u}\right). \end{aligned} \quad (14)$$

After replacing the expressions (14) in (7), AUC can be computed numerically. As explained before, the characteristic functions $\psi_0(u)$ and $\psi_1(u)$ can be expanded into Taylor series, in order to circumvent the numerical problems associated to the principal value appearing in (7). The following results are then obtained:

$$\text{AUC} = \frac{1}{2} + \frac{1}{2} \sum_{k, l \geq 0} c_{k, l} \text{sgn}\left(\sum_{n=1}^N \beta_n (l_n - k_n)\right), \quad (15)$$

where $k = (k_1, \dots, k_N)$, $l = (l_1, \dots, l_N)$ and

$$c_{k,l} = e^{-h-2Nf} \frac{f^{\sum_{n=1}^N k_n} \prod_{n=1}^N (f + h\alpha_n)^{l_n}}{\prod_{n=1}^N k_n! \prod_{n=1}^N l_n!}. \quad (16)$$

The determination of AUC by (15) requires high computational cost for large values of f , h , N . In this case, it is interesting to use the approximated AUC derived in [2]. This is the purpose of the next section.

6. LIKELIHOOD-GENERATING FUNCTION

When the test statistics T is the log-likelihood ratio, the moment-generating functions of T under hypotheses H_0 and H_1 satisfy the relation $M_0(u+1) = M_1(u)$ where $M_i(u) = E[e^{uT}|H_i]$, [2]. This allows to express AUC as follows:

$$\text{AUC} = \frac{1}{2} + \frac{1}{2i\pi} \mathcal{P} \int_{\mathbb{R}} e^{-4\pi^2 u^2} e^{2i\pi u} \frac{H(u)}{u} du, \quad (17)$$

where $H(u) = G(-2i\pi u - \frac{1}{2}) - G(2i\pi u + \frac{1}{2})$ and $G(u)$ is a so-called likelihood-generating function defined as:

$$G(u) = \frac{\log M_0(u + \frac{1}{2})}{(u - \frac{1}{2})(u + \frac{1}{2})}. \quad (18)$$

Since the exponential factor in (17) falls off rapidly as u increases, $H(u)$ can be expanded in a Taylor series around $u = 0$:

$$H(u) = 2 \sum_{k=0}^{\infty} \frac{G^{(2k)}(0)}{(2k)!} \left(2i\pi u + \frac{1}{2}\right)^{2k}, \quad (19)$$

which shows that AUC depends on the derivatives of $G(u)$ at $u = 0$. Assume that $G(u)$ can be approximated by a linear function near the origin. The Taylor series (19) can be truncated after $n = 1$ which yields:

$$\text{AUC} \simeq \text{AUC}_a = \frac{1}{2} + \frac{1}{2} \text{erf}\left(\frac{1}{2} \sqrt{2G(0)}\right), \quad (20)$$

where $\text{erf}(\cdot)$ is the error function.

It is interesting to note that for a Gaussian distributed log-likelihood ratio, $G(u)$ is constant and the approximation (20) is an equality. Indeed, the mean and variance of T under hypothesis H_0 are necessarily linked by the relation $m_0 = -\frac{1}{2}\sigma_0^2$, the moment-generating function under hypothesis H_0 is $M_0(u) = \exp\left(\frac{\sigma_0^2}{2}(u^2 - u)\right)$ and $G(u) = \frac{\sigma_0^2}{2}$.

In the low-flux imagery problem defined in section 4, the moment generating functions of T can be computed under hypotheses H_0 and H_1 . This allows to compute the corresponding likelihood-generating function:

$$G(u) = \frac{-uh - h/2 - Nf + f \sum_{n=1}^N e^{\beta_n(u+1/2)}}{(u - \frac{1}{2})(u + \frac{1}{2})} \quad (21)$$

Consequently, the AUC can be approximated by (20) with:

$$G(0) = 4 \left(\frac{h}{2} + Nf - f \sum_{n=1}^N \sqrt{1 + \frac{h}{f} \alpha_n} \right) \quad (22)$$

A first order expansion of $G(0)$ for large values of f yields:

$$G(0) = \frac{h^2}{8f} \sum_{n=1}^N \alpha_n^2 + o(1/f) \quad (23)$$

This result is in perfect agreement with the snr obtained for the high flux detection problem defined in [5] as follows:

$$H_0 : X_n \sim \mathcal{N}(f, f), \quad H_1 : X_n \sim \mathcal{N}(f + h\alpha_n, f). \quad (24)$$

Note that the likelihood-generating function introduced before can also be used to derive a lower bound for the AUC. More precisely, the following result can be obtained [2]:

$$\text{AUC} \geq \text{AUC}_\ell = 1 - \frac{1}{2} \exp\left(-\frac{G(0)}{2}\right). \quad (25)$$

This lower bound is valid without approximation as soon as T is a log-likelihood ratio. It provides a lower bound for AUC which depends on $G(0)$ only.

Note that the bound AUC_ℓ and the approximation AUC_a increase when $G(0)$ gets larger. The parameter $G(0)$ can be viewed as a signal to noise ratio for the detection problem (12).

Figure 1 shows the variations of AUC, its approximation AUC_a and the lower bound AUC_ℓ as a function of parameter f . This figure has been obtained with $N = 1$, $h = 1$. The summation in (15) has been appropriately truncated to ensure an accurate value of AUC. The validity of the approximation is clearly demonstrated. However, the lower bound appears to be very loose for the problem (12).

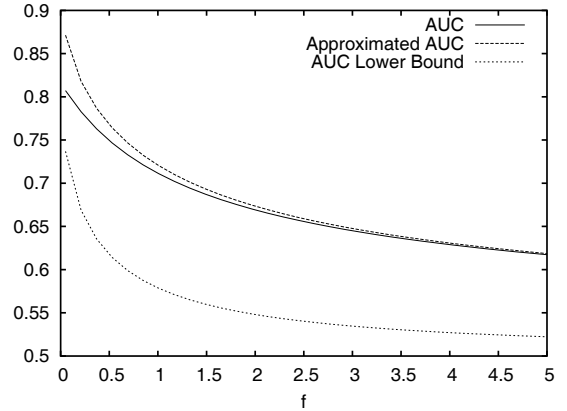


Fig. 1. AUC, AUC_a and AUC_ℓ versus f for $N = 1$.

Figures 2 and 3 show the variations of AUC_a as a function of f for $h = 1$ and various sets of parameters $\{N, \alpha_n\}$. The parameters α_n in the two figures correspond to two different sampling schemes of the same point spread function (PSF). For each figure, the increase of N results in an oversampling of the same PSF.

The detection performance increases when f decreases as expected (see (22)). The performance also increases when N decreases. This last result must be analyzed by taking into account the renormalisation of the α_n for each value of N . Moreover, for the same value of N , the performance is better in figure 3 than figure 2. This can be explained by (23). Indeed, for the same value of N , the energy $E_\alpha = \sum_{n=1}^N \alpha_n^2$ is higher in figure 3 than in figure 2. The last simulation depicted in figure 4 shows the variations of AUC_a as a function of h for $f = 1$. AUC_a is obviously an increasing function of h .

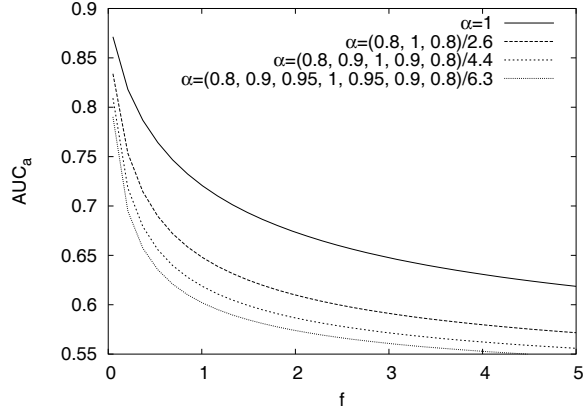


Fig. 2. AUC_α versus f for different N ; $E_\alpha = 1, 0.33, 0.20, 0.14$.

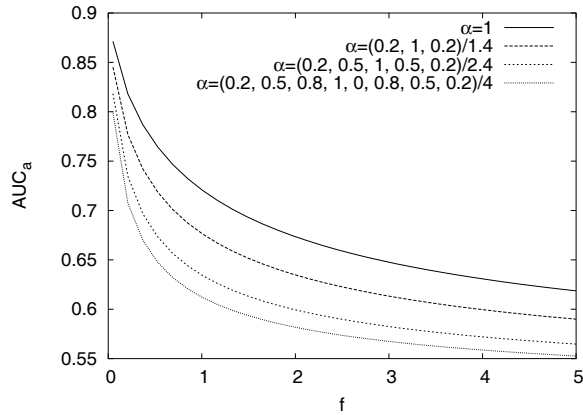


Fig. 3. AUC_α versus f for different N ; $E_\alpha = 1, 0.55, 0.27, 0.17$.

7. CONCLUSION

This paper has provided new results for the detection of changes in a Poisson distribution for low-flux imagery. The performance of the Neyman Pearson detector for this problem is difficult to obtain analytically. We have proposed to measure the detection performance by the area under the ROC (AUC). An accurate approximation of the AUC has been derived. This allowed to define a so-called signal to noise ratio for the low-flux detection problem.

8. APPENDIX A

This appendix derives the expressions of AUC_1 and AUC_2 for a test statistic distributed according to a Poisson distribution. Denote as $a(i, j) = \frac{\lambda_0^i \lambda_1^j}{i! j!}$. The indices of the sums $\sum_{k=0}^j \sum_{i=0}^k a(i, j)$ and $\sum_{k=0}^j a(i, j)$ belong to the lower triangle and the diagonal of the square $\{0, \dots, k\} \times \{0, \dots, k\}$. By summing on the diagonals

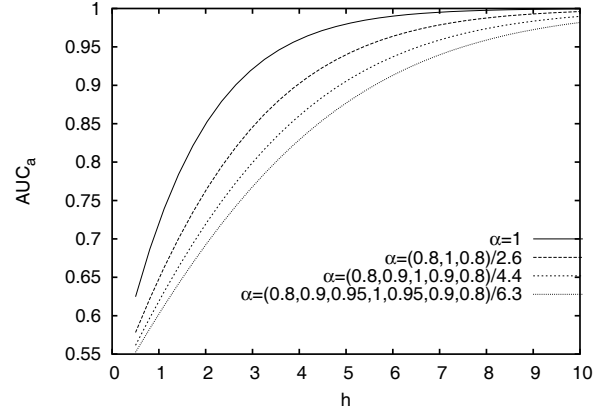


Fig. 4. AUC_α versus h for different N .

of this square, the following results can be obtained:

$$\begin{aligned} e^{(\lambda_0 + \lambda_1)} AUC_1 &= \sum_{l=0}^{\infty} \sum_{i=0}^{\infty} a(i+l, i) = \sum_{l=0}^{\infty} \lambda_0^l \left(\sum_{i=0}^{\infty} \frac{(\lambda_0 \lambda_1)^i}{(i+l)! i!} \right) \\ &= \sum_{l=0}^{\infty} \left(\frac{\lambda_0}{\lambda_1} \right)^{l/2} I_l(2\sqrt{\lambda_0 \lambda_1}), \end{aligned}$$

where $I_l(z)$ is the modified Bessel function of the first kind of order l [4]. The second term AUC_2 can be computed similarly since

$$e^{(\lambda_0 + \lambda_1)} AUC_2 = \sum_{i=0}^{\infty} a(i, i) = I_0(2\sqrt{\lambda_0 \lambda_1}). \quad (26)$$

Combining the previous results, the AUC can be expressed as follows

$$\begin{aligned} AUC &= 1 - e^{-(\lambda_0 + \lambda_1)} \sum_{l=0}^{\infty} \left(\frac{\lambda_0}{\lambda_1} \right)^{l/2} I_l(2\sqrt{\lambda_0 \lambda_1}) + \\ &\quad \frac{1}{2} e^{-(\lambda_0 + \lambda_1)} I_0(2\sqrt{\lambda_0 \lambda_1}). \quad (27) \end{aligned}$$

9. REFERENCES

- [1] H. L. Van Trees, *Detection, Estimation, and Modulation Theory, Part I: Detection, Estimation, and Linear Modulation Theory*. New York: Wiley, 1968.
- [2] H. H. Barrett, C. K. A. Tu, and E. Clarkson, "Objective assessment of image quality. ROC metrics, ideal observers, and likelihood-generating functions," *J. Opt. Soc. Am.*, vol. 15, pp. 1520–1535, June 1998.
- [3] F. Goudail, N. Roux, and P. Refregier, "Performance parameters for detection in low-flux coherent images," *Opt. Lett.*, vol. 28, pp. 81–83, Jan. 2003.
- [4] M. Abramowitz and I. Stegun, *Handbook of Mathematical Functions*. New York: Dover, 1965.
- [5] A. Ferrari, O. Michel, and C. Aime, "Analysis of flux variance detection in Poisson processes. Application to direct detection of extra-solar planet," in *Proc. Workshop on Physics in Signal and Image Processing*, (Grenoble, France), Jan. 2003.